Icarus 251 (2015) 145–163

Contents lists available at ScienceDirect

Icarus

journal homepage: www.elsevier.com/locate/icarus

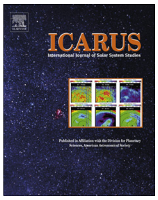

Mars Express measurements of surface albedo changes over 2004–2010

M. Vincendon [a,*], J. Audouard [a], F. Altieri [b], A. Ody [a,c]

[a] Institut d'Astrophysique Spatiale, Université Paris Sud, 91405 Orsay, France
[b] INAF, IAPS, Rome, Italy
[c] Laboratoire de Géologie de Lyon, 69622 Villeurbanne, France

ARTICLE INFO

Article history:
Received 10 July 2014
Revised 10 October 2014
Accepted 17 October 2014
Available online 4 November 2014

Keywords:
Mars, surface
Mars, climate
Mars, atmosphere
Photometry
Radiative transfer

ABSTRACT

The pervasive Mars dust is continually transported between the surface and the atmosphere. When on the surface, dust increases the albedo of darker underlying rocks and regolith, which modifies climate energy balance and must be quantified. Remote observation of surface albedo absolute value and albedo change is however complicated by dust itself when lifted in the atmosphere. Here we present a method to calculate and map the bolometric solar hemispherical albedo of the martian surface using the 2004–2010 OMEGA imaging spectrometer dataset. This method takes into account aerosols radiative transfer, surface photometry, and instrumental issues such as registration differences between visible and near-IR detectors. Resulting albedos are on average 17% higher than previous estimates for bright surfaces while similar for dark surfaces. We observed that surface albedo changes occur mostly during the storm season due to isolated events. The main variations are observed during the 2007 global dust storm and during the following year. A wide variety of change timings are detected such as dust deposited and then cleaned over a martian year, areas modified only during successive global dust storms, and perennial changes over decades. Both similarities and differences with previous global dust storms are observed. While an optically thin layer of bright dust is involved in most changes, this coating turns out to be sufficient to mask underlying mineralogical near-IR spectral signatures. Overall, changes result from apparently erratic events; however, a cyclic evolution emerges for some (but not all) areas over long timescales.

1. Introduction

The changing appearance of Mars to human eyes has long been documented from Earth and satellite observations. Major changes are related to atmospheric and polar phenomena occurring on daily to seasonal scales: formation, movement and dissipation of ice and dust clouds; advance and retreat of polar caps (Leighton et al., 1969; Baum, 1974; Pleskot and Miner, 1981). Changes also occur at the ice-free surface on multiple timescales. These variations are essentially due to modification of the surface coating by fine bright dust over the larger-grained darker underlying material (Pollack and Sagan, 1967; Sagan et al., 1973). Episodic removal of large amount of bright dust due to short-lived strong winds occurs during the storm season (De Mottoni et al., 1982; Lee, 1986; Szwast et al., 2006; Cantor, 2007; Geissler et al., 2010). Progressive dust erosion is also observed under the effect of (1) topographically and thermally driven horizontal wind gusts (Sagan et al., 1973; Christensen, 1988; Szwast et al., 2006; Cantor et al., 2006), (2) dust devils (Geissler, 2005; Greeley et al., 2005, 2006; Cantor et al., 2006) and (3) dark sand saltation (Sullivan et al., 2008; Geissler et al., 2010; Vaughan et al., 2010). Subsequent settling of dust (Landis and Jenkins, 2000) then brightens dark surfaces. Local (Geissler et al., 2010) or regional (Szwast et al., 2006) horizontal transport of dust by episodic strong winds is observed during the storm season, as well as gradual accumulation of dust linked with topography (Veverka et al., 1977; Geissler, 2012). Regional fallout also temporarily blankets certain areas of Mars such as Syrtis Major during global dust storm decay (Christensen, 1988; Szwast et al., 2006; Cantor, 2007). Other minor contributors to surface albedo change include horizontal movements of dark sand grains under strong winds (Geissler et al., 2010; Bridges et al., 2012; Chojnacki et al., in press), gravity-driven mass-movements (Sullivan et al., 2001; Treiman, 2003; Schorghofer and King, 2011), defrosting processes modifying underling ice-free surface (Dundas et al., in press), and slope flow potentially involving water (Malin et al., 2006; McEwen et al., 2011).

The existence and degree of persistence of albedo modification depends on the competition between erosion and accumulation mechanisms, which relative intensity depends on season, year, location, and surface properties (De Mottoni et al., 1982; Lee, 1986; Szwast et al., 2006; Sullivan et al., 2008; Geissler et al.,

---

[*] Corresponding author. Fax: +33 1 69 85 86 75.
E-mail address: mathieu.vincendon@u-psud.fr (M. Vincendon).

http://dx.doi.org/10.1016/j.icarus.2014.10.029
0019-1035/© 2014 Elsevier Inc. All rights reserved.

2010). Overall, dark regions seem to rapidly recover their pre-storm albedo value (Pleskot and Miner, 1981; Christensen, 1988; Cantor, 2007; Vincendon et al., 2009), suggestive of a relatively perennial albedo distribution, in agreement with the persistence of Mars main albedo markings over time (Christensen, 1988; Geissler, 2005; Szwast et al., 2006). However, significant local long-term differences, lasting over decades, have also been reported (Pollack and Sagan, 1967; Baum, 1974; De Mottoni et al., 1982; Capen, 1976; James et al., 1996; Bell et al., 1999; Erard, 2000; Geissler, 2005), as well as progressive movements of albedo frontiers (Veverka et al., 1977; Chaikin et al., 1981; Geissler, 2005). Assessing the irreversible versus cyclic nature of these changes requires further albedo change monitoring.

Surface albedo changes and associated dust reservoir redistribution could alter current climate via temperatures and winds modification (Kahre et al., 2005; Cantor, 2007; Fenton et al., 2007; Montmessin et al., 2007). Albedo is indeed a key parameter controlling the energy budget at the surface and must be properly modeled in energy balance codes and global climate models (Forget et al., 1999; Kieffer, 2013), as well as during thermal inertia retrievals (Mellon et al., 2000; Putzig et al., 2005; Fergason et al., 2006; Audouard et al., 2014). Variations in dust coating also modify the distribution and apparent spectral properties of exposed surface material detected by remote sensors (Singer and Roush, 1983; Christensen, 1988; Poulet et al., 2007; Rice et al., 2011; Carrozzo et al., 2012). Understanding the timing and mechanisms associated with current dust deposition and removal is also of importance for future mission planning, as persistent settling of dust alters robotic and instrumental performances (Landis and Jenkins, 2000; Smith et al., 2006; Kinch et al., 2007; Vaughan et al., 2010; Drube et al., 2010; Lemmon et al., 2015).

Estimating absolute surface reflectance values and associated time variations from orbit is tricky. First, remote observations of the surface are performed with variable illumination and viewing geometries depending on spacecraft, season and latitude, which results in phase effects of both the atmosphere and the surface. Second, observations of the surface are performed through the atmosphere which contains varying amounts of dust and clouds. Third, the reflectance at all solar wavelengths and in all directions must be accounted for to get precise constraints about the energy balance at the surface. Finally, the time sampling of observations is also of importance to assess the duration of detected changes. The OMEGA imaging spectrometer onboard Mars Express measures wavelengths from early visible to near-IR. Global coverage of the planet with repeated observations of several areas with variable photometric and atmospheric conditions have been obtained over more than 3 Mars years (MY), from early 2004 (late MY26) to mid-2010 (mid MY30). Additional observations with a restricted wavelength range are ongoing (2014, MY32). This time range includes the 2007 (MY28) global dust storm (GDS), whose timing significantly differs from the 2001 (MY25) storm monitored by Mars Global Surveyor (MGS). The spatial resolution of OMEGA varies between 0.3 and 5 km, which provides a compromise between global coverage and details at the surface. In this study, we calculate surface hemispherical bolometric albedo using OMEGA data and report surface changes observed over the last 10 years at non polar latitudes (60°S–60°N).

2. Method

2.1. OMEGA data characteristics and selection

The OMEGA dataset consist of hyperspectral images of the surface and atmosphere of Mars obtained from orbit. OMEGA collects the reflected sunlight between 0.35 and 5.1 μm over 352 spectral channels divided into three detectors, with a contribution of thermal emission for wavelengths greater than 3 μm. Ground photometric calibration was performed for a targeted accuracy better than 20% in absolute terms (Bonello et al., 2005). Comparison of OMEGA data with HRSC and telescopic observations in the visible and near-IR during the mission showed that the absolute accuracy is in fact better than 10% in that range (McCord et al., 2007). The calibration of the 0.36–1.07 μm channel (hereafter "visible channel") has been recently revisited, with a high level of confidence for wavelengths $\geqslant$0.43 μm and $\leqslant$0.95 μm (Bellucci et al., 2006; Carrozzo et al., 2012). The photometric response of the 0.93–2.69 μm channel (hereafter "near-IR channel") is checked for each orbit via an on-board calibration procedure and remained stable during the mission (Ody et al., 2012). We will only consider wavelengths $\geqslant$1.08 μm for this channel to retain data with the highest signal to noise ratio. While atmospheric gas absorptions can be corrected for wavelengths $\leqslant$2.5 μm (see e.g. Langevin et al., 2007), a changing water vapor feature followed by a broad saturated CO_2 gas band makes it difficult to recover surface reflectance beyond 2.5 μm. The photometric response of the 2.53–5.09 μm channel had varied over the mission, making use of this channel for absolute reflectance measurements more complex (Jouglet et al., 2009). This channel also contains numerous broad, partly saturated gas absorptions (for wavelengths $\leqslant$2.9 μm and $\geqslant$4 μm), and covers a wavelength range for which the solar flux is negligible (see Section 2.2) while the thermal emission from the surface is significant: it will thus not be used in this work.

The spatial resolution at the surface ranges from 0.3 km to 5 km depending on Mars Express altitude on its elliptical polar orbit. The spatial dimensions of images correspond to a few hundreds to thousands of pixels in the orbit direction and to 16–128 pixels perpendicularly to the orbit (the lower the spacecraft altitude is, the smaller the image width is). Two co-aligned units cover the solar range with distinct telescopes and operating modes: the push broom method for the visible channel (with a line of pixels perpendicular to the orbit) and the whisk broom technology for the near-IR channel (with one pixel scanning the surface perpendicularly to the orbit). These two acquisition methods and the fact that the visible channel is adjacent but physically separated from the near-IR one produce some differences in the spatial coverage of the two channels. First, the field of view is larger for the visible channel compared to the near-IR channel, especially in the "*Y*" direction (i.e., along the spacecraft track), which partly lowers the actual spatial resolution when we combine both detectors. Second, a misalignment between these two channels results in spatial registration inconsistency of typically a few pixels. This misalignment changes from observation to observation (Carrozzo et al., 2012) and within a given observation. We co-register both channels by maximizing the correlation between the 0.9 μm and 1.1 μm measurements with a changing shift value within a given observation. In the "*X*" direction (i.e., perpendicular to the spacecraft track) the misalignment ranges from 2 pixels (for 16 pixels wide observations) to 5–6 pixels (for 128 pixels wide observations). In the *Y* direction the shift is greater than 3 pixels. It depends on the spacecraft altitude and velocity which vary as Mars Express orbit is elliptical. Thus, the *Y* misalignment can change by several pixels within a given observation. This procedure can however not be easily achieved automatically for cubes including targets other than the surface (typically, cubes observing both the surface and the atmosphere at the limb). These observations will thus be considered but as lower quality data.

Viewing conditions vary within the dataset. Emission (emergence) angles are near-nadir for most observations but can be up to 90° when pointing drifts toward limb observations. Solar zenith angles (also referred as incidence angles) ranges from zenith (0°) to terminator (90°) depending on local time, season and latitude. Due